2-5-2009

Hygroscopic Behavior and Liquid-Layer Composition of Aerosol Particles Generated from Natural and Artificial Seawater

Matthew E. Wise
Arizona State University, mawise@cu-portland.edu

Evelyn J. Freney
Arizona State University

Corey A. Tyree
Arizona State University

Jonathan O. Allen
Arizona State University

Scot T. Martin
Harvard University

See next page for additional authors

Authors
Matthew E. Wise, Evelyn J. Freney, Corey A. Tyree, Jonathan O. Allen, Scot T. Martin, Lynn M. Russell, and Peter R. Buseck

Hygroscopic behavior and liquid-layer composition of aerosol particles generated from natural and artificial seawater

Matthew E. Wise,[1] Evelyn J. Freney,[1] Corey A. Tyree,[2] Jonathan O. Allen,[2,3] Scot T. Martin,[4] Lynn M. Russell,[5] and Peter R. Buseck[1]

Received 19 May 2008; revised 18 September 2008; accepted 7 November 2008; published 5 February 2009.

[1] Sea-salt aerosol (SSA) particles affect the Earth's radiative balance and moderate heterogeneous chemistry in the marine boundary layer. Using conventional and environmental transmission electron microscopes (ETEM), we investigated the hygroscopic growth and liquid-layer compositions of particles generated from three types of aqueous salt solutions: sodium chloride, laboratory-synthesized seawater (S-SSA particles), and natural seawater (N-SSA particles). Three levels of morphological change were observed with the ETEM as the laboratory-generated particles were exposed to increasing relative humidity (RH). The first level, onset of observable morphological changes, occurred on average at 70, 48, and 35% RH for the NaCl, S-SSA, and N-SSA particles, respectively. The second level, rounding, occurred at 74, 66, and 57% RH for NaCl, S-SSA, and N-SSA particles, respectively. The third level, complete deliquescence, occurred at 75% RH for all particles. Collected ambient SSA particles were also examined. With the exception of deliquescence, they did not exhibit the same hygroscopic characteristics as the NaCl particles. The ambient particles, however, behaved most similarly to the synthesized and natural SSA particles, although the onset of morphological change was slightly higher for the S-SSA particles. We used energy-dispersive X-ray spectrometry to study the composition of the liquid layer formed on the S-SSA and N-SSA particles. The layer was enriched in Mg, S, and O relative to the solid particle core. An important implication of these results is that $MgSO_4$-enriched solutions on the surface of SSA particles may be the solvents of many heterogeneous reactions.

Citation: Wise, M. E., E. J. Freney, C. A. Tyree, J. O. Allen, S. T. Martin, L. M. Russell, and P. R. Buseck (2009), Hygroscopic behavior and liquid-layer composition of aerosol particles generated from natural and artificial seawater, *J. Geophys. Res.*, *114*, D03201, doi:10.1029/2008JD010449.

1. Introduction

[2] Sea-salt aerosol (SSA) particles influence the radiative balance in the marine environment directly by scattering light [e.g., *Murphy et al.*, 1998] and indirectly by serving as cloud condensation nuclei (CCN) [e.g., *Mason*, 2001]. The direct radiative effect due to SSA particles is estimated to be -1.5 to -5 W/m^2 [*Haywood et al.*, 1999]. The indirect radiative effect arising from the cloud-nucleating abilities of SSA particles over the Indian Ocean is estimated to be -7 ± 4 W/m^2 [*Vinoj and Satheesh*, 2003].

[3] Heterogeneous reactions on SSA particles have also been reported. Depending on how water is bound to the particles, gas-phase HNO_3 can react with a probability of at least an order of magnitude greater than for reaction on dry NaCl particles [*De Haan and Finlayson-Pitts*, 1997]. It is therefore important to determine which portion of the SSA particles initiates water uptake and to determine its chemical composition. Using this information, experiments designed to determine gas-phase reaction probabilities at appropriate gas/liquid solution interfaces can be carried out.

[4] The compositions of atmospheric particles greatly influence their hygroscopic properties, which in turn affect their ability to scatter light, act as efficient CCN, and catalyze heterogeneous reactions. At a characteristic relative humidity (RH), a pure salt particle (such as NaCl) takes up water to form a solution droplet in a process termed deliquescence [*Martin*, 2000]. As the RH increases past the deliquescence RH (DRH), the particle grows hygroscopically to maintain equilibrium with the water vapor. If the RH decreases, the particle loses water and eventually reforms crystals (efflorescence) at an RH value (ERH) significantly lower than the DRH. The water uptake characteristics of many atmospherically relevant salts such as

[1] School of Earth and Space Exploration and Department of Chemistry and Biochemistry, Arizona State University, Tempe, Arizona, USA.
[2] Chemical Engineering Department, Arizona State University, Tempe, Arizona, USA.
[3] Civil and Environmental Engineering Department, Arizona State University, Tempe, Arizona, USA.
[4] School of Engineering and Applied Sciences, Harvard University, Cambridge, Massachusetts, USA.
[5] Scripps Institution of Oceanography, University of California, La Jolla, California, USA.

0148-0227/09/2008JD010449

NaCl (DRH ~ 75% and ERH ~ 45%) have been studied [i.e., *Biskos et al.*, 2006; *Martin*, 2000; *Tang and Munkelwitz*, 1984, 1994; *Wise et al.*, 2005; *Weiss and Ewing*, 1999].

[5] Although SSA particles contain mostly NaCl, they also contain a variety of inorganic components that can affect their hygroscopic properties. On the basis of the composition of natural seawater, the ionic composition of dry, freshly emitted SSA particles is 55.04% (w/w) Cl^-, 30.61% Na^+, 7.68% SO_4^{2-}, and 3.69% Mg^{2+} [*Pilson*, 1998]. SSA particles can also contain a significant fraction of organic compounds [*O'Dowd et al.*, 2004], some of which partition to the air/water interface of oceanic bubbles during ascent. Single-particle measurements of natural marine aerosol particles indicate that on the order of 10% of the particle mass is organic matter [*Middlebrook et al.*, 1998]. Thus researchers studying the hygroscopic properties of SSA particles must generate complex particles in the laboratory or perform ambient studies in which evolution of SSA particles is uncertain.

[6] Many investigators studied the deliquescence and efflorescence transitions of SSA particles using both experimental and modeling techniques. Using particles generated from the atomization of artificial seawater containing no organic molecules (using the procedure of *Kester et al.* [1967]), *Cziczo et al.* [1997] reported that the infrared spectra of S-SSA particles contained strong water bands at RH values as low as 2%. They attributed the existence of water at low RH possibly to a supersaturated liquid or to solid Mg^{2+} salt hydrates (e.g., $MgCl_2 \cdot 6H_2O$). Furthermore, they saw observable water uptake at RH values > 50% and substantial water uptake at RH values between 70 and 80%.

[7] *Lee and Hsu* [2000] showed that particles atomized from collected seawater fully deliquesced by 73% RH. They also detected water associated with the particles at 0% RH, which they attributed to water molecules bound to $MgCl_2$. Furthermore, they detected water uptake beginning at ~55% RH. However, they were unable to determine which portions of the SSA particles initiated water uptake. Finally, using a modeling technique, *Ming and Russell* [2001] showed that SSA particles containing a mixture of insoluble organic molecules, soluble organic molecules, and inorganic compounds were expected to take up more water than NaCl from 50 to 75% RH. These studies provided valuable insights into the hygroscopic properties of SSA particles.

[8] The experimental studies described above were unable to visually confirm the portions of the SSA particles initiating water uptake. Therefore electron microscopes have been used to study the morphological changes in particles arising from exposure to water vapor and other atmospheric gases. Several investigators used an environmental scanning electron microscope (ESEM) to determine the hygroscopic properties of individual inorganic particles [*Ebert et al.*, 2002] and mixed-phase inorganic particles [*Hoffman et al.*, 2004]. *Krueger et al.* [2003] used an ESEM to monitor the morphological changes of nebulized SSA particles that were exposed to mixtures of gas-phase H_2O and HNO_3, and *Laskin et al.* [2005] studied the formation of nitrates from ambient calcite and SSA particles.

[9] The ESEM can be used to study the morphological changes of individual aerosol particles as they are exposed to atmospheric gases. However, it has limited spatial resolution and is restricted to imaging surface features. In contrast, a transmission electron microscope (TEM) can resolve features down to fractions of a nanometer and can be used to investigate surfaces in cross section. Recently, an environmental transmission electron microscope (ETEM) was used to study the morphological changes associated with water uptake by individual inorganic particles generated in the laboratory. *Wise et al.* [2007] and *Semeniuk et al.* [2007] studied the water uptake of individual NaCl-bearing aerosol particles collected from industrial pollution plumes, and from clean and polluted marine environments. *Wise et al.* [2008] utilized laboratory-generated NaCl particles to show that a significant amount of water is reversibly associated with NaCl particles (generated with an atomizer) prior to deliquescence. These studies confirmed that water uptake by multiphase particles occurs at a lower RH than the DRH of their component phases, as expected [*Martin*, 2000].

[10] The current work advances our prior work on water uptake of NaCl and ambient sea-salt particles to study the water uptake of sea-salt particles generated in the laboratory. Here we report on changes in the morphology of particles generated from pure NaCl, laboratory-synthesized seawater, and natural seawater solutions during exposure to RH values between 0 and 100%. The changes are compared to those observed for ambient SSA particles, collected from clean and polluted marine environments [*Wise et al.*, 2007; *Semeniuk et al.*, 2007]. We also investigated the effects of two particle-generation methods (atomization and foam-bubble bursting) on hygroscopic properties.

2. Experimental

2.1. Aqueous Media Used for Particle Generation

[11] Pure NaCl particles were generated from a solution created by dissolving NaCl in water. Laboratory-synthesized SSA (S-SSA) particles were generated from a solution created by dissolving 58.9% NaCl, 30.8% $MgCl_2 \cdot 6H_2O$, 9.71 Na_2SO_4, and 0.588% $NaHCO_3$ (by weight) in water. The laboratory-synthesized seawater solution was based on that used by *Lewis and Schwartz* [2004] but was modified to obtain the correct pH by including $NaHCO_3$. Solutions were made from reagent-grade materials with doubly distilled, deionized water. To generate natural SSA particles (N-SSA), we used a sample of seawater collected from the Scripps Institution of Oceanography pier in La Jolla, CA. The sample was collected from an ocean depth of 20 cm to avoid sampling the surface microlayer. The salinity of the seawater sample was 33.4‰ and chlorophyll, which is a proxy for organic matter, was 0.2 mg/m^3 (data courtesy of the Southern California Coastal Observing System, www.sccoos.org). The procedure used to collect and preserve the seawater sample is given by *Tyree et al.* [2007]. The natural seawater sample was stored at 0°C in the dark and used within 24 hours of collection.

[12] The ambient SSA particles were collected from clean (Cape Grim Baseline Air Pollution Station) and polluted (San Diego, CA) marine environments. These particles were chosen because their compositions and hygroscopic properties were described in detail by *Wise et al.* [2007] (Figure 1, particles 4 and 5) and *Semeniuk et al.* [2007] (Figure 1, particles 2 and 3), they can be used in this study as a tool for comparison. Because the particles were collected in a marine

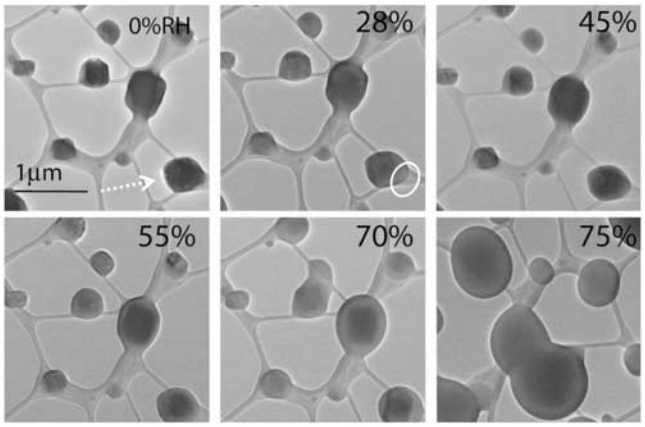

Figure 1. Images of S-SSA particles as the RH was raised to 75%. The particles were generated through atomization. The circle highlights the onset of morphological change. The image at 75% is not of the same field of view.

environment, each particle contained a significant fraction of sodium chloride. In addition to sodium chloride, the individual particles contained insoluble materials such as calcium sulfate [*Wise et al.*, 2007] (particle 4), soluble compounds such as sodium nitrate [*Wise et al.*, 2007] (particle 5), mixed cation sulfate coatings [*Semeniuk et al.*, 2007] (particle 2), and magnesium-rich chloride coatings [*Semeniuk et al.*, 2007] (particle 3).

2.2. Particle Generation and Collection Methods

[13] We employed two methods to create the particles used for hygroscopic growth measurements. In the first method, particles were generated by bubbling air through the solutions described in section 2.1 to produce foam droplets. This procedure was used to mimic the natural production of SSA particles over the ocean. A full description of this generation method is given by *Tyree et al.* [2007]; we briefly describe it here. First, a precleaned glass column (height 60 cm, width 15 cm) was filled with 7.2 L of solution. A precleaned fine-pore diffuser attached to a stainless steel tube was submerged to approximately 1 cm above the bottom of the column. The top of the glass column was then covered with a cone-shaped piece of aluminum foil, and 3.4 L/min (superficial velocity of 0.33 cm/s) of air was passed through the diffuser to produce bubbles with mean diameters of 230 μm (standard deviation 80 μm). Furthermore, the surface of the solutions were approximately 90% covered by rafts of foam bubbles approximately 0.5 cm thick.

[14] The aerosol particles produced by foam bubbles bursting were sampled at ~2.5 L/min through a diffusion dryer (TSI Model 3062) using an MPS-3 microanalysis particle sampler (California Instruments, Inc.). This process reduced the ambient RH to between ~45 and 65%. The MPS-3 sampler allowed the particles to be collected directly onto Cu-mesh TEM grids with an ultrathin carbon film on a holey carbon support film (Ted Pella, Inc. # 01822).

[15] We also generated particles by the atomization of the solutions using a TSI Model 3076 Atomizer. Following atomization (using N_2 gas at ~3 L/min), the particles were sampled (at ~2.5 L/min) through the diffusion dryer using the MPS-3 particle sampler. The particles were then collected directly onto TEM grids.

2.3. Hygroscopic Behavior of the Particles

[16] Water-uptake experiments were carried out using a 200-kV FEI Tecnai F20 TEM fitted with a differentially pumped environmental cell. *Wise et al.* [2005] described the ETEM and the procedure developed to study the hygroscopic properties of aerosol particles. The procedure was slightly modified by *Wise et al.* [2007]. The hygroscopic behavior of each particle presented here was studied over the range 0 to 100% RH. The process of recording images of each particle at a given RH took ~5 min.

[17] Prior to each ETEM experiment, the accuracy of RH measurement was verified by measuring the DRH of laboratory-synthesized NaCl particles. The DRH for these particles was 75 ± 2%, in agreement with the known DRH of NaCl [i.e., *Biskos et al.*, 2006; *Cziczo et al.*, 1997; *Ebert et al.*, 2002; *Richardson and Snyder*, 1994; *Tang and Munkelwitz*, 1993; *Wise et al.*, 2005]. Although the accuracy of the RH measurements using the ETEM was ≤2%, their day-to-day precision was ≤1%.

[18] In this manuscript we present data on the hygroscopic behavior of at least 30 particles of each type. Because of space considerations, we illustrate the hygroscopic behavior of large groups of particles with images of selected particles. The hygroscopic behavior of the particles shown, however, is representative of the particles studied using the ETEM.

[19] We use three terms to describe the effects of increasing RH on particle morphology. The "onset of morphological change" is noted when the first morphological change can be observed by simple visual inspection. It is inferred that the first changes in morphology are due to water on the surface of the particles which facilitate ion movement. "Rounding" is noted when the angular corners of a square particle become fully rounded. At this point, the particles have taken up a significant amount of water but have yet to fully deliquesce. Final deliquescence is determined by complete dissolution of the solid particle.

2.4. Conventional TEM Analyses

[20] Bright-field images and energy-dispersive X-ray spectrometry (EDS) measurements were recorded for specific particles using a Philips CM200 TEM operated at 200 kV. The microscope was used to provide morphological and chemical information on particles after ETEM analyses. Detailed analysis of the particles first involved imaging with spot size 1 (25 nm) to document different phases within each particle. After imaging the particles, we performed a qualitative chemical analysis of each phase using EDS with spot size 5 (6.0 nm) at intervals of 3 s. The spectra were collected using ES Vision software.

3. Results and Discussion

3.1. Hygroscopic Properties of Model SSA Particles Observed Using the ETEM

[21] We reported observations of the changes that pure NaCl particles undergo as RH is increased from 0 to 100% using the ETEM [*Wise et al.*, 2005, 2008].

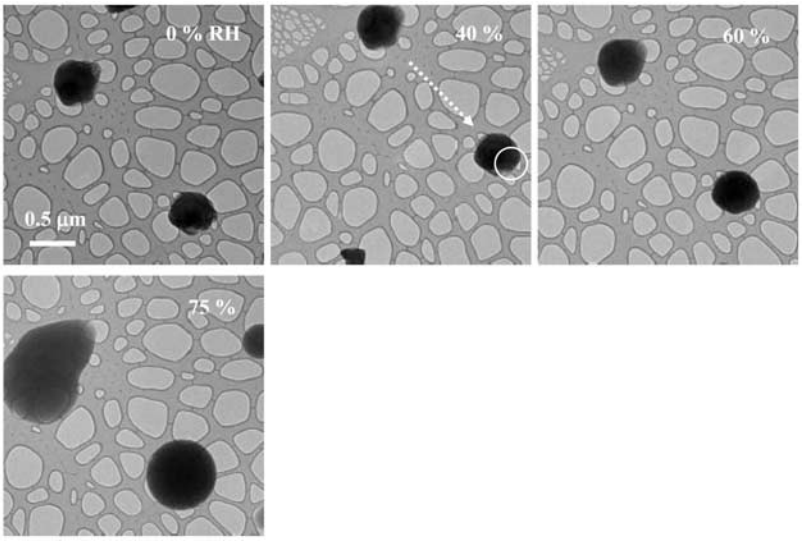

Figure 2. Images of a submicron N-SSA particle (highlighted with the dashed arrow) as RH was raised to 75%. The particle was generated by foam-bubble bursting. The circle highlights the onset of morphological change prior to deliquescence.

Laboratory-synthesized SSA particles and particles generated from a natural seawater sample, however, contain species other than NaCl. An ~0.5-μm S-SSA particle (highlighted with an arrow in Figure 1) exhibited onset of morphological change at 28% RH. As the RH was increased to 55%, the particle edges rounded, and at 75% RH the particle fully deliquesced. The other particles in Figure 1 behaved similarly, although morphological changes were observed at slightly different RH values.

[22] At 40% RH the onset of morphological change occurred on the surface of a 0.56-μm N-SSA particle (highlighted with a dashed arrow in Figure 2). As the RH was increased to 60% the particle edges became rounder, and at 75% RH the particle fully deliquesced. The other N-SSA particle imaged in Figure 2 exhibited similar hygroscopic characteristics.

[23] Using the observations described above for numerous S-SSA and N-SSA particles, we plot in Figure 3 the RH at which we detected the onset of morphological change, rounding, and full deliquescence versus particle diameter (geometric). As a basis for comparison, we also included observations from previously studied NaCl particles (Figure 3a) [*Wise et al.*, 2005, 2008]. Table 1 summarizes the RH values at which the three levels of morphological change occurred for NaCl, S-SSA, N-SSA, and ambient SSA particles.

[24] For most NaCl particles, the first changes in morphology (open squares and circles) occurred between 65 and 75% RH. Similarly, *Ebert et al.* [2002] found that water adsorption on the surface of NaCl particles occurred at ~75% RH with their ESEM apparatus. In addition, *Wise et al.* [2008] using the ETEM showed that a significant amount of water is reversibly associated with NaCl particles prior to deliquescence when they are supported by a substrate. To explain the observations, a phase rule was derived which allowed for the coexistence of liquid, solid, and vapor for the binary $NaCl/H_2O$ system across a range of RH values. Although the substrate-supported NaCl particles picked up water prior to deliquescence, the RH at which the NaCl particles fully deliquesced was consistent with the literature value of ~75% (horizontal line) for particles greater than 40 nm in diameter.

[25] The RH values at which we detected the onset of morphological change, rounding, and deliquescence are plotted versus S-SSA particle size in Figure 3b. The onset for S-SSA particles occurred between 15 and 65% RH. Between 55 and 70% RH S-SSA particles became rounded, and at ~75% the particles fully deliquesced. *Zhao et al.* [2006] studied the hygroscopic properties of $MgSO_4$ aerosol particles using FTIR spectroscopy and found that below ~42.3% RH they showed no sign of water uptake with increasing RH. As the RH was increased past ~42.3%, the particles gradually took up water. At 53.7% RH full deliquescence was indicated. The S-SSA particles in our study contained a significant amount of Mg and SO_4 ions. It is inferred that at the onset of morphological change, the S-SSA particles began to take up water. Therefore from 15 to 50% RH they appear to exhibit similar hygroscopic characteristics as the $MgSO_4$ particles in the work of *Zhao et al.* [2006]. Thus $MgSO_4$ could have influenced the initial water uptake by S-SSA particles. The S-SSA particles in our study also contained a significant amount of Mg and Cl ions. At 298 K, the DRH of $MgCl_2$ is ~33%. Therefore it is also plausible that $MgCl_2$ could have influenced the initial water uptake by S-SSA particles.

[26] The RH values at which different morphological changes were observed for N-SSA particles are plotted in Figure 3c. The onset of morphological change for N-SSA particles occurred between 10 and 65% RH. The onset for N-SSA particles occurred at systematically lower RH values than for NaCl and at approximately the same RH as the S-SSA particles. The RH range where particle rounding occurred for the N-SSA particles was also similar to that observed for S-SSA particles. All N-SSA particles fully deliquesced by 75% RH. Although the hygroscopic properties of NaCl and S-SSA particles were not influenced by

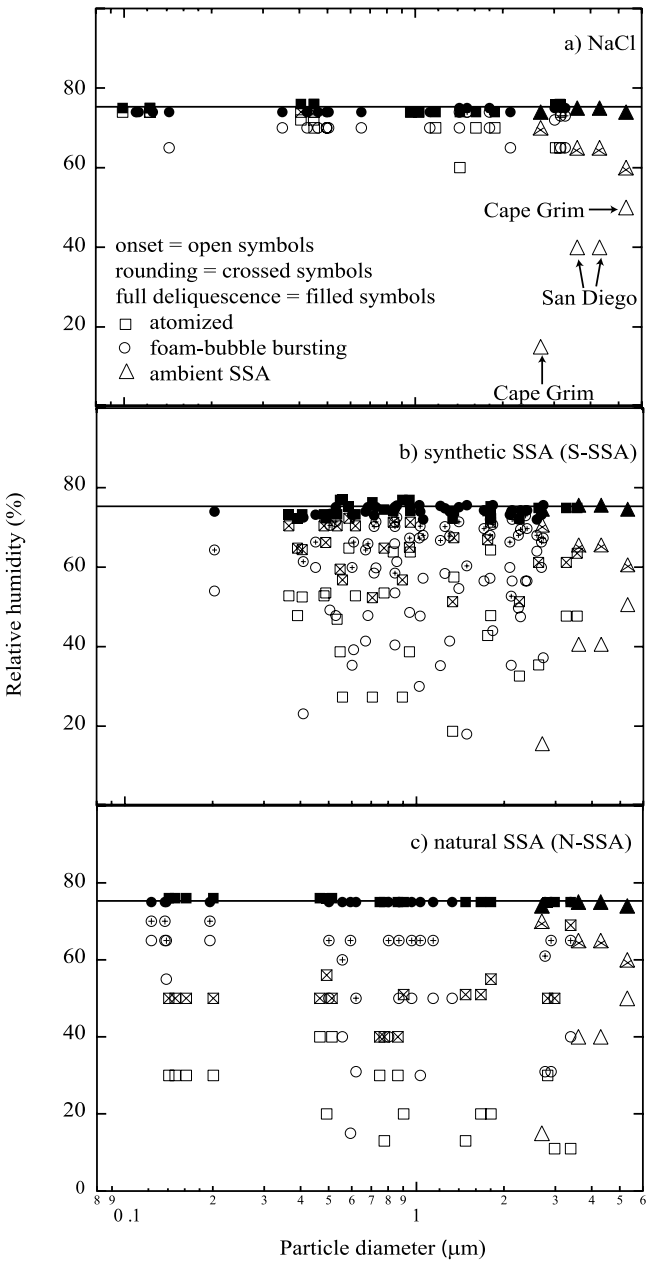

Figure 3. Relative humidity at which we observed the onset of morphological change, particle rounding, and deliquescence for (a) NaCl particles, (b) S-SSA, and (c) N-SSA as a function of size. For comparison, water-uptake experiments previously performed on ambient SSA particles are included.

whether they had been generated by atomization (squares) or foam-bubble bursting (circles), N-SSA particles generated using the atomizer generally began to change at RH values lower than generated by foam-bubble bursting. This observation is consistent with inhibited water uptake to N-SSA formed by foam-bubble bursting which are expected to be enriched in organics relative to the bulk seawater.

3.2. Comparison of Model SSA Particles With Select Ambient Particles

[27] A goal of this study is to determine whether model SSA particles behave similarly to ambient SSA particles. Therefore we plot in Figure 3 the RH at which four ambient SSA particles exhibited morphological changes (triangles). The ambient SSA particles had initial changes in particle morphology between 15 and 50% RH, significantly lower than the NaCl particles. Ambient SSA, like N-SSA particles, contain a complex mixture of inorganic ions and organic molecules. Moreover, ambient SSA particles interact with gas-phase species in the atmosphere, thereby changing their composition from natural seawater. Similar to N-SSA particles, ambient SSA particles took up water at RH values far below full deliquescence, and the RH range where onset of morphological changes occurred was similar. Between 55 and 70% RH, the RH values at which N-SSA particles became rounded were comparable to those of the ambient SSA particles (i.e., rounding between 40 and 70% RH).

[28] The N-SSA particles generated using the bubble-bursting method (denoted with circles in Figure 3) have the most similar hygroscopic characteristics to ambient SSA. Particles generated using the atomizer (denoted with squares in Figure 3) have slightly different hygroscopic characteristics. However, the RH at which particle rounding occurs for S-SSA, N-SSA, and ambient SSA occurs is comparable.

3.3. Composition of Liquid Coating of Partially Deliquesced Particles

[29] The S-SSA, N-SSA, and ambient SSA particles exhibited significant morphological changes and water uptake with increasing RH. The composition of the solution surrounding the particles at the point where they became rounded is of special interest because the liquid layer surrounding the particles has the ability to catalyze heterogeneous reactions in the atmosphere [e.g., *De Haan and Finlayson-Pitts*, 1997; *Hu and Abbatt*, 1997].

[30] To determine the ions in the liquid layer, we exposed freshly generated N-SSA particles to a RH of 71% in the ETEM (Figure 4, image i). After the particles were imaged, the water vapor was pumped away. Because the surface tension between the liquid layer and the substrate drew the liquid away from the solid core of the particle (see Figure 4, image i), it separately recrystallized (indicated by the dashed arrow in Figure 4, image ii). In order to determine composition, we transferred the particles to a TEM (Philips CM200) with the ability to perform EDS measurements unavailable in the ETEM.

Table 1. Summary of the RH Values at Which Morphological Changes Occur for NaCl, S-SSA, N-SSA, and Ambient SSA

	NaCl		S-SSA		N-SSA		
	Bubble Bursting	Atomizer	Bubble Bursting	Atomizer	Bubble Bursting	Atomizer	Ambient SSA
Onset of morphology change (RH, %)	69 ± 3[a] (16)[b]	71 ± 4 (15)	48 ± 12 (37)	46 ± 13 (25)	45 ± 14 (17)	25 ± 9 (17)	36 ± 15 (4)
Particle rounding (RH, %)	74 ± 1 (5)	74 ± 1 (3)	67 ± 5 (37)	67 ± 7 (25)	65 ± 5 (16)	50 ± 7 (17)	65 ± 4 (4)
Full deliquescence (RH, %)	74 ± 1 (20)	74 ± 1 (15)	74 ± 2 (37)	74 ± 2 (25)	75 ± 1 (17)	75 ± 1 (17)	75 ± 1 (4)

[a]Standard deviation of the RH values at which changes occur for the particles regardless of size.
[b]Parenthesized values indicate the number of particles studied.

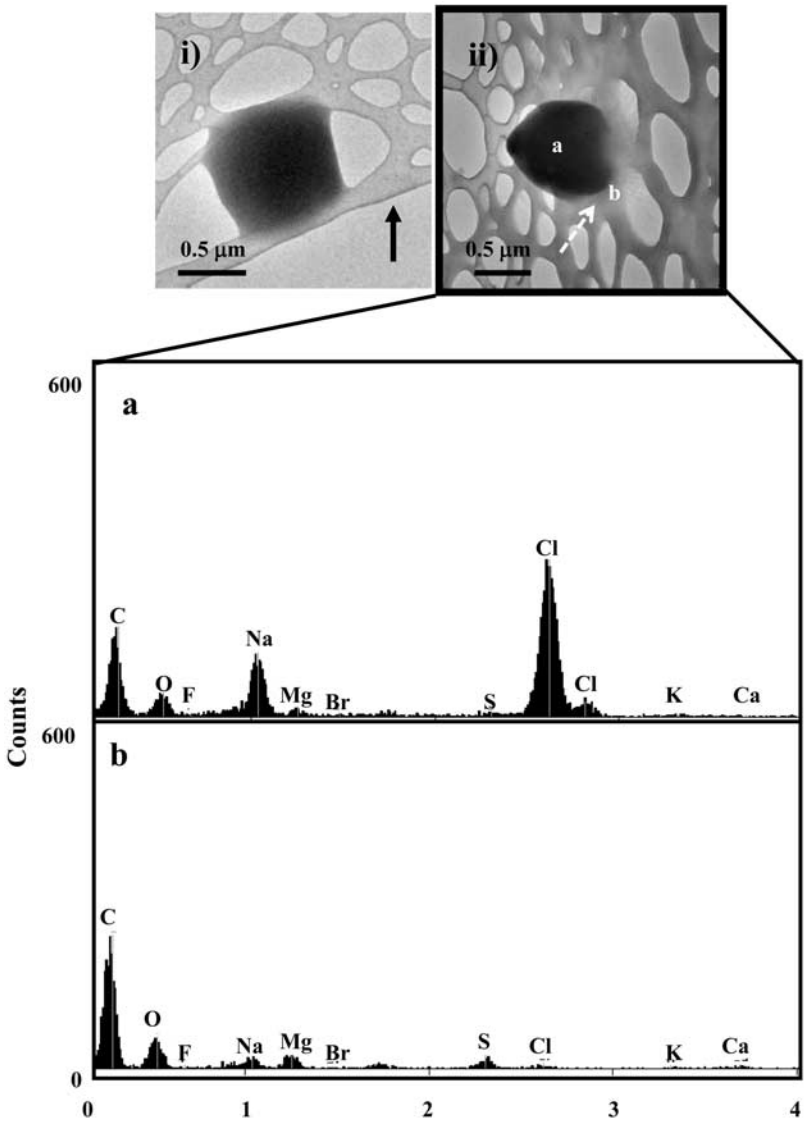

Figure 4. (i) Image taken with the ETEM of an N-SSA particle (generated by foam-bubble bursting) at 74% RH. (ii) Image taken with the Philips CM200 microscope of a different N-SSA particle (generated by foam-bubble bursting) that had been previously exposed to water vapor in the ETEM. The lower case letters denote the areas in Figure 4ii where the EDS measurements were obtained. The particle imaged in Figure 4i is different from the one imaged in Figure 4ii because of the difficulty in finding specific particles after transferring grid.

[31] To determine differences in composition, we obtained EDS measurements of both the (a) particle core and (b) surrounding residue. The spectrum collected from the particle core contained Na and Cl as well as C, O, and Mg peaks. The positions of other elements in natural seawater are labeled in spectrum 1; however, their signals were not strong enough to be detected above the noise level. The spectrum collected from the residue contained the same elements as the particle core, with an additional peak attributed to S.

[32] We performed the same type of analysis with an S-SSA particle (Figure 5, image i). The spectrum collected from the particle core contained Na and Cl as well as a small Mg peak. The spectrum collected from the residue contained the same elements as the particle core, with additional peaks attributed to S and O. The EDS spectra of single SSA particles (Figures 4 and 5) show that the outer layer of material contains Mg, Cl, and S whereas the EDS spectra of the particle cores show Na and Cl. These results follow well with predictions made for sea-salt crystallization by *Harvie et al.* [1980]. Mg and K salts crystallize last in the sequence during dehydration because of their higher solubility in water.

[33] Our results confirm that when sea-salt particles dry crystalline NaCl makes up the core while more soluble salts are concentrated toward the particle surface. For this reason it can be expected that dry sea-salt particles consist of layers with their most soluble species at the surface. These more soluble species are responsible for taking up water at RH lower than pure NaCl (see Figures 1 and 2). *Liu et al.* [2008] also reported, using FT-IR spectroscopy, water uptake at RH values in the range of 30 to 50% for sea-salt particles. The

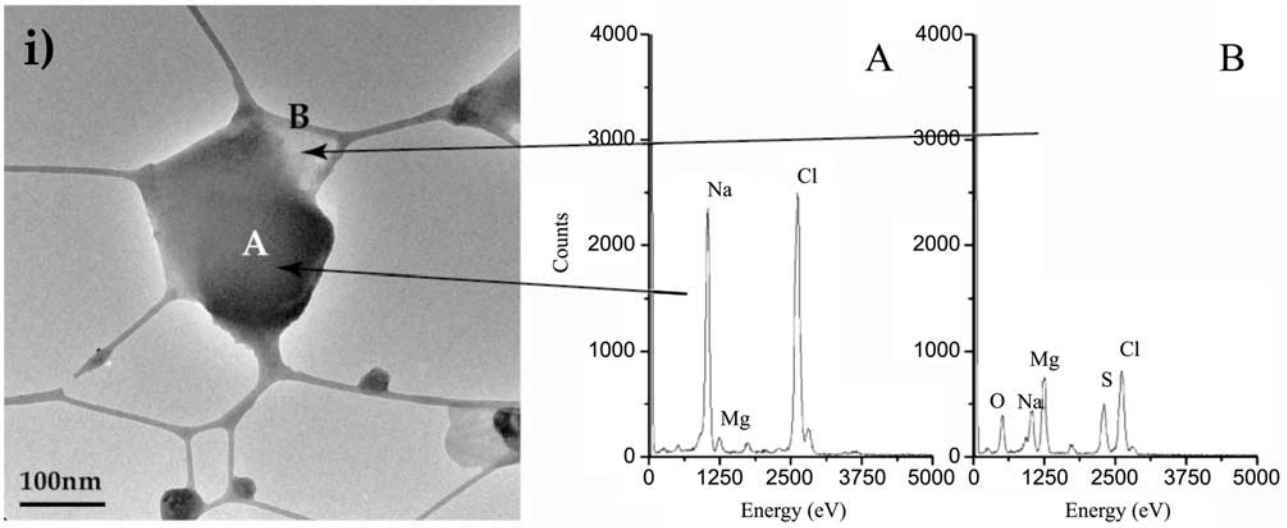

Figure 5. (i) Image taken with the Philips CM200 microscope of a S-SSA particle generated from bubble bursting. The upper case letters denote areas where EDS spectra were taken.

uptake of water prior to full deliquescence observed for the natural and synthetic sea-salt particles can be explained if we consider the evaporation of seawater. This type of heterogeneous core-shell particle morphology has been reported in a number of studies on particles composed of binary, internally mixed salts where the solubilities are significantly different [*Ge et al.*, 1996; *Hoffman et al.*, 2004].

4. Conclusions

[34] Our results provide strong visual evidence on how the hygroscopic properties of NaCl, S-SSA, N-SSA, and ambient SSA particles differ. In a previous manuscript, we found that NaCl particles took up a significant amount of water at RH values slightly lower than the accepted deliquescence RH of 75%. The water uptake in the NaCl particles was due to a surface effect rather than a composition effect. In contrast, the S-SSA particles in the current study showed water uptake for increasing RH due to a compositional effect (S-SSA contain Cl^-, Na^+, SO_4^{2-}, Mg^{2+}, and HCO_3^-). The RH range for which we observed water uptake is in agreement with that seen by *Cziczo et al.* [1997], and we are in agreement with *Cziczo et al.* [1997] on the RH values at which full deliquescence occurs. Therefore our results provide visual evidence confirming the effects of increasing RH on the water content of NaCl and SSA particles.

[35] We found that there were no differences in the hygroscopic properties of NaCl and S-SSA particles generated by either atomization or foam-bubble bursting. By comparison, there was a slight difference in the onset of morphological changes and rounding for N-SSA particles depending on the method of particle production. The N-SSA particles that showed the most similar hygroscopic characteristics to ambient SSA particles were those formed by foam-bubble bursting. The similarity in hygroscopic characteristics may have occurred because the OC was preferentially taken up at the air/water interface during bubbling and foam formation. Therefore researchers utilizing seawater samples containing OC may wish to consider employing foam-bubble bursting to produce their particles.

[36] Many reactive processes that occur on SSA particles depend on how water is associated with the particles. For example, *De Haan and Finlayson-Pitts* [1997] found that the reaction probability for HNO_3 with S-SSA particles occurred at least an order of magnitude faster than for reaction on NaCl particles. They attributed this difference to the presence of hygroscopic crystalline hydrates such as $MgCl_2 \cdot 2H_2O$. We saw significant water uptake by our S-SSA and N-SSA particles, suggesting increases in the capacity for aqueous chemistry at the air-particle interface at RH values significantly below that of full deliquescence.

[37] Our results suggest that $MgSO_4$ (perhaps hydrated) play an important role in the initial water uptake of both S-SSA and N-SSA particles. Thus the minor ionic components of seawater, namely Mg^{2+} and SO_4^{2-}, play a more important role in water uptake at intermediate RH values than their seawater concentrations might suggest. This conclusion is supported by EDS measurements that show the liquid layer associated with S-SSA and N-SSA particles prior to deliquescence is enriched in Mg, S, and O relative to the particle core.

[38] **Acknowledgments.** This manuscript is based on a work supported by the National Science Foundation under grant 0304213 from the Division of Atmospheric Chemistry. Any opinions, findings, and conclusions or recommendations expressed in this material are those of the authors and do not necessarily reflect the views of the National Science Foundation. We gratefully acknowledge the use of the facilities at the John M. Cowley Center for High Resolution Electron Microscopy within the LeRoy Eyring Center for Solid State Science at Arizona State University. In particular, we thank Karl Weiss, John Wheatley (deceased), Grant Baumgardner, Renu Sharma, and Peter Crozier for their assistance with developing our ETEM technique.

References

Biskos, G., A. Malinowski, L. M. Russell, P. R. Buseck, and S. T. Martin (2006), Nanosize effect on the deliquescence and the efflorescence of sodium chloride particles, *Aerosol Sci. Technol.*, *40*, 97–106.

Cziczo, D. J., J. B. Nowak, J. H. Hu, and J. P. D. Abbatt (1997), Infrared spectroscopy of model tropospheric aerosols as a function of relative humidity: Observation of deliquescence and crystallization, *J. Geophys. Res.*, *102*, 18,843–18,850.

De Haan, D. O., and B. J. Finlayson-Pitts (1997), Knudsen cell studies of the reaction of gaseous nitric acid with synthetic sea salt at 298 K, *J. Phys. Chem. A*, *101*, 9993–9999.

Ebert, M., M. Inerle-Hof, and S. Weinbruch (2002), Environmental scanning electron microscopy as a new technique to determine the hygroscopic behaviour of individual aerosol particles, *Atmos. Environ.*, *36*, 5909–5916.

Ge, Z. Z., A. S. Wexler, and M. V. Johnston (1996), Multicomponent aerosol crystallization, *J. Colloid Interface Sci.*, *183*, 68–77.

Harvie, C. E., J. H. Weare, L. A. Hardie, and H. P. Eugster (1980), Evaporation of seawater—Calculated mineral sequences, *Science*, *208*, 498–500.

Haywood, J. M., V. Ramaswamy, and B. J. Soden (1999), Tropospheric aerosol climate forcing in clear-sky satellite observations over the oceans, *Science*, *283*, 1299–1303.

Hoffman, R. C., A. Laskin, and B. J. Finlayson-Pitts (2004), Sodium nitrate particles: Physical and chemical properties during hydration and dehydration, and implications for aged sea salt aerosols, *J. Aerosol Sci.*, *35*, 869–887.

Hu, J. H., and J. P. D. Abbatt (1997), Reaction probabilities for N_2O_5 hydrolysis on sulfuric acid and ammonium sulfate aerosols at room temperature, *J. Phys. Chem. A*, *101*, 871–878.

Kester, D. R., I. W. Duedall, D. N. Connors, and R. M. Pytkowic (1967), Preparation of artificial seawater, *Limnol. Oceanogr.*, *12*, 176–179.

Krueger, B. J., V. H. Grassian, M. J. Iedema, J. P. Cowin, and A. Laskin (2003), Probing heterogeneous chemistry of individual atmospheric particles using scanning electron microscopy and energy-dispersive X-ray analysis, *Anal. Chem.*, *75*, 5170–5179.

Laskin, A., M. J. Iedema, A. Ichkovich, E. R. Graber, I. Taraniuk, and Y. Rudich (2005), Direct observation of completely processed calcium carbonate dust particles, *Faraday Discuss.*, *130*, 453–468.

Lewis, E. R., and S. E. Schwartz (2004), *Sea Salt Aerosol Production: Mechanisms, Methods, Measurements, and Models: A Critical Review*, AGU, Washington, D. C.

Lee, C. T., and W. C. Hsu (2000), The measurement of liquid water mass associated with collected hygroscopic particles, *J. Aerosol Sci.*, *31*, 189–197.

Liu, Y. Y., Z. Desyaterlk, P. Gassman, H. Wang, and A. Laskin (2008), Hygroscopic behavior of substrate-deposited particles studied by micro-FT-IR spectroscopy and complementary methods of particle analysis, *Anal. Chem.*, *80*(3), 633–642.

Martin, S. T. (2000), Phase transitions of aqueous atmospheric particles, *Chem. Rev.*, *100*, 3403–3454.

Mason, B. J. (2001), The role of sea-salt particles as cloud condensation nuclei over the remote oceans, *Q. J. R. Meteorol. Soc.*, *127*, 2023–2032.

Middlebrook, A. M., D. M. Murphy, and D. S. Thomson (1998), Observations of organic material in individual marine particles at Cape Grim during the First Aerosol Characterization Experiment (ACE 1), *J. Geophys. Res.*, *103*, 16,475–16,483.

Ming, Y., and L. M. Russell (2001), Predicted hygroscopic growth of sea salt aerosol, *J. Geophys. Res.*, *106*, 28,259–28,274.

Murphy, D. M., J. R. Anderson, P. K. Quinn, L. M. McInnes, F. J. Brechtel, S. M. Kreidenweis, A. M. Middlebrook, M. Posfai, D. S. Thomson, and P. R. Buseck (1998), Influence of sea-salt on aerosol radiative properties in the Southern Ocean marine boundary layer, *Nature*, *392*, 62–65.

O'Dowd, C. D., M. C. Facchini, F. Cavalli, D. Ceburnis, M. Mircea, S. Decesari, S. Fuzzi, Y. J. Yoon, and J. P. Putaud (2004), Biogenically driven organic contribution to marine aerosol, *Nature*, *431*, 676–680.

Pilson, M. E. Q. (1998), *An Introduction to the Chemistry of the Sea*, Prentice-Hall, Upper Saddle River, N. J.

Richardson, C. B., and T. D. Snyder (1994), A study of heterogeneous nucleation in aqueous-solutions, *Langmuir*, *10*, 2462–2465.

Semeniuk, T. A., M. E. Wise, S. T. Martin, L. M. Russell, and P. R. Buseck (2007), Water uptake characteristics of individual atmospheric particles having coatings, *Atmos. Environ.*, *41*, 6225–6235.

Tang, I. N., and H. R. Munkelwitz (1984), An investigation of solute nucleation in levitated solution droplets, *J. Colloid Interface Sci.*, *98*, 430–438.

Tang, I. N., and H. R. Munkelwitz (1993), Composition and temperature-dependence of the deliquescence properties of hygroscopic aerosols, *Atmos. Environ.*, *27*, 467–473.

Tang, I. N., and H. R. Munkelwitz (1994), Aerosol phase-transformation and growth in the atmosphere, *J. Appl. Meteorol.*, *33*, 791–796.

Tyree, C. A., V. M. Hellion, O. A. Alexandrova, and J. O. Allen (2007), Foam droplets generated from natural and artificial seawaters, *J. Geophys. Res.*, *112*, D12204, doi:10.1029/2006JD007729.

Vinoj, V., and S. K. Satheesh (2003), Measurements of aerosol optical depth over Arabian Sea during summer monsoon season, *Geophys. Res. Lett.*, *30*(5), 1263, doi:10.1029/2002GL016664.

Weiss, D. D., and G. E. Ewing (1999), Water content and morphology of sodium chloride aerosol particles, *J. Geophys. Res.*, *104*, 21,275–21,285.

Wise, M. E., G. Biskos, S. T. Martin, L. M. Russell, and P. R. Buseck (2005), Phase transitions of single salt particles studied using a transmission electron microscope with an environmental cell, *Aerosol Sci. Technol.*, *39*, 849–856.

Wise, M. E., T. A. Semeniuk, R. T. Bruintjes, S. T. Martin, L. M. Russell, and P. R. Buseck (2007), Hygroscopic behavior of NaCl-bearing natural aerosol particles using environmental transmission electron microscopy, *J. Geophys. Res.*, *112*, D10224, doi:10.1029/2006JD007678.

Wise, M. E., S. T. Martin, L. M. Russell, and P. R. Buseck (2008), Water uptake by NaCl particles prior to deliquescence and the phase rule, *Aerosol Sci. Technol.*, *42*, 281–294.

Zhao, L., Y. Zhang, Z. Wei, H. Cheng, and X. Li (2006), Magnesium sulfate aerosols studied by FTIR spectroscopy: Hygroscopic properties, supersaturated structures, and implications for seawater aerosols, *J. Phys. Chem. A*, *110*, 951–958.

J. O. Allen and C. A. Tyree, Chemical Engineering Department, Arizona State University, P.O. Box 876006, Tempe, AZ 85287-6006, USA.

P. R. Buseck, E. J. Freney, and M. E. Wise, School of Earth and Space Exploration and Department of Chemistry and Biochemistry, Arizona State University, Bateman Physical Sciences Center F-wing, Room 686, Tempe, AZ 85287-1404, USA. (matthew.wise@colorado.edu)

S. T. Martin, School of Engineering and Applied Sciences, Harvard University, Pierce Hall, Room 122, 29 Oxford Street, Cambridge, MA 02138, USA.

L. M. Russell, Scripps Institution of Oceanography, University of California, San Diego, 9500 Gilman Drive, La Jolla, CA 92093, USA.